World Journal of Gastroenterology

Online Submissions: http://www.wjgnet.com/esps/
wjg@wjgnet.com
doi:10.3748/wjg.v18.i47.7048

World J Gastroenterol 2012 December 21; 18(47): 7048-7055
ISSN 1007-9327 (print) ISSN 2219-2840 (online)

BRIEF ARTICLE

Hepatic focal nodular hyperplasia in children: Imaging features on multi-slice computed tomography

Qing-Yu Liu, Wei-Dong Zhang, Dong-Ming Lai, Ying Ou-yang, Ming Gao, Xiao-Feng Lin

Qing-Yu Liu, Ming Gao, Xiao-Feng Lin, Department of Radiology, Sun Yat-sen Memorial Hospital, Sun Yat-sen University, Guangzhou 510120, Guangdong Province, China
Wei-Dong Zhang, Department of Radiology, Cancer Center, Sun Yat-sen University, Guangzhou 510060, Guangdong Province, China
Dong-Ming Lai, Department of General Surgery, Sun Yat-sen Memorial Hospital, Sun Yat-sen University, Guangzhou 510120, Guangdong Province, China
Ying Ou-yang, Department of Pediatrics, Sun Yat-sen Memorial Hospital, Sun Yat-sen University, Guangzhou 510120, Guangdong Province, China
Author contributions: Liu QY designed the study and wrote the manuscript; Zhang WD, Gao M and Lin XF contributed to the analysis and interpretation of imaging data; Lai DM and Ou-yang Y contributed to the interpretation of clinical data.
Correspondence to: Qing-Yu Liu, PhD, Department of Radiology, Sun Yat-sen Memorial Hospital, Sun Yat-sen University, 107 Yan Jiang Xi Road, Guangzhou 510120, Guangdong Province, China. liu.qingyu@163.com
Telephone: +86-20-81332243 Fax: +86-20-81332702
Received: September 13, 2012 Revised: October 31, 2012
Accepted: November 11, 2012
Published online: December 21, 2012

Abstract

AIM: To retrospectively analyze the imaging features of hepatic focal nodular hyperplasia (FNH) in children on dynamic contrast-enhanced multi-slice computed tomography (MSCT) and computed tomography angiography (CTA) images.

METHODS: From September 1999 to April 2012, a total of 218 cases of hepatic FNH were confirmed by either surgical resection or biopsy in the Sun Yat-sen Memorial Hospital of Sun Yat-sen University and the Cancer center of Sun Yat-sen University, including 12 cases (5.5%) of FNH in children (age ⩽ 18 years old). All the 12 pediatric patients underwent MSCT. We retrospectively analyzed the imaging features of FNH lesions, including the number, location, size, margin, density of FNH demonstrated on pre-contrast and contrast-enhanced computed tomography (CT) scanning, central scar, fibrous septa, pseudocapsule, the morphology of the feeding arteries and the presence of draining vessels (portal vein or hepatic vein).

RESULTS: All the 12 pediatric cases of FNH had solitary lesion. The maximum diameter of the lesions was 4.0-12.9 cm, with an average diameter of 5.5 ± 2.5 cm. The majority of the FNH lesions (10/12, 83.3%) had well-defined margins. Central scar (10/12, 83.3%) and fibrous septa (11/12, 91.7%) were commonly found in children with FNH. Central scar was either isodense (n = 7) or hypodense (n = 3) on pre-contrast CT images and showed progressive enhancement in 8 cases in the equilibrium phase. Fibrous septa were linear hypodense areas in the arterial phase and isodense in the portal and equilibrium phases. Pseudocapsule was very rare (1/12, 8.3%) in pediatric FNH. With the exception of central scars and fibrous septa within the lesions, all 12 cases of pediatric FNH were homogenously enhanced on the contrast-enhanced CT images, significantly hyperdense in the arterial phase (12/12, 100.0%), and isodense in the portal venous phase (7/12, 58.3%) and equilibrium phase (11/12, 91.7%). Central feeding arteries inside the tumors were observed on CTA images for all 12 cases of FNH, whereas no neovascularization of malignant tumors was noted. In 9 cases (75.0%), there was a spoke-wheel shaped centrifugal blood supply inside the tumors. The draining hepatic vein was detected in 8 cases of pediatric FNH. However, the draining vessels in the other 4 cases could not be detected. No associated hepatic adenoma or hemangioma was observed in the livers of the 12 pediatric cases.

CONCLUSION: The characteristic imaging appearances of MSCT and CTA may reflect the pathological and hemodynamic features of pediatric FNH. Dynamic multi-phase MSCT and CTA imaging is an effective method for diagnosing FNH in children.

Key words: Focal nodular hyperplasia; Liver; Children; Benign hepatic lesions; X-ray; Computed tomography

Peer reviewer: Dr. Koike Naoto, Department of Surgery, Seirei Sakura Citizen Hospital, 2-36-2 Ebaradai, Chiba 2858765, Japan

Liu QY, Zhang WD, Lai DM, Ou-yang Y, Gao M, Lin XF. Hepatic focal nodular hyperplasia in children: Imaging features on multi-slice computed tomography. *World J Gastroenterol* 2012; 18(47): 7048-7055 Available from: URL: http://www.wjgnet.com/1007-9327/full/v18/i47/7048.htm DOI: http://dx.doi.org/10.3748/wjg.v18.i47.7048

INTRODUCTION

Hepatic focal nodular hyperplasia (FNH) is the second most common benign liver tumor after hemangioma, occurring in approximately 3%-5% of the general population[1]. The mechanism for the pathogenesis of FNH is unclear, although it may be caused by a proliferative response to local vascular abnormalities[2]. FNH is most common in adult females, with a female to male ratio of 2-4:1[1,3], whereas it is rare in children. If a focal hypervascular liver lesion is accidentally detected in children during imaging, it is important to differentiate FNH from other malignant lesions to avoid unnecessary surgical resection. Since FNH is a slow growing tumor without malignant transformation and is rarely accompanied by the complications of hemorrhage or rupture, conservative "wait and see" strategy is recommended for asymptomatic children[4]. Surgical treatment would be considered only for symptomatic pediatric patients, patients with increasing size of FNH, or patients in whom malignancy cannot be rule out confidently[5-7].

Multi-slice spiral computed tomography (CT) technology has rapidly developed since the clinical application of 16-slice spiral CT was introduced in 2001. Multi-slice computed tomography (MSCT) (16 slices, 64 slices or 128 slices) features a fast scanning speed (the time required for a single tube rotation is sub-second) and is ideal for assessing pediatric patients. With MSCT, dynamic multiphase scanning is allowed in a very short period of time, and increased detection and characterization of focal liver lesion can be achieved[2]. In addition, the ability of MSCT to acquire data with "isotropic voxel" makes high-quality two- or three-dimensional vascular reconstruction images possible[3]. To the best of our knowledge, there are few reports on the imaging features of FNH in children[4,8,9]. The previous imaging procedure most often utilized for the assessment of the hemodynamic characteristics of FNH was angiography, which is invasive and labor-intensive. Studies that analyze the imaging characteristics of FNH in children on MSCT images and the angioarchitecture of pediatric FNH on computed tomography angiography (CTA) have not reported in the literature. This paper retrospectively reviewed the imaging features of MSCT in 12 cases of FNH in children.

MATERIALS AND METHODS

Patients

The database of the Sun Yat-sen Memorial Hospital of Sun Yat-sen University and the Cancer Center of Sun Yat-sen University was searched from September 1999 to April 2012, and 218 cases of hepatic FNH confirmed by surgical resection or biopsy were identified. Out of the 218 cases, there were 12 cases (5.5%) of FNH in children (aged ⩽ 18 years).

Out of the 12 pediatric cases, 8 were males and 4 were females. The age of the patients ranged from 2 years old to 18 years old, with an average of 12.1 ± 6.4 years. Four pediatric cases presented with abdominal pain, 2 cases presented with palpable abdominal masses, 1 case presented with upper abdominal discomfort, and the other 5 asymptomatic cases were discovered accidentally during imaging check-up for related reasons. In 1 patient, hemangiomas were found in the right shoulder and nasal alae when the diagnosis of hepatic FNH was established. All 12 cases were negative for hepatitis B surface antigen markers and for tumor markers, such as alpha-fetoprotein (AFP), carcinoembryonic antigen 125, and carbohydrate antigen 19-9. All the 12 pediatric patients did not have a history of malignancy or stem cell transplantation.

Imaging protocols

MSCT examinations were performed on either a 64-slice spiral CT scanner (Sensation 64, Siemens Medical Solutions, Erlangen, Germany) or a 16-slice spiral CT scanner (Brilliance™ 16, Philips Medical Systems, Best, The Netherlands) in all 12 pediatric patients. The CT scan parameters were as follows: a tube voltage of 120 kV, an effective tube current of 85-200 mAs, and collimation of 64 mm × 0.6 mm or 16 mm × 0.75 mm. After pre-contrast scanning images were obtained, multiphase contrast-enhanced CT scan was performed after intravenous administration of nonionic contrast material of Iopamidol (370 mgI/mL, Bracco, Milan, Italy) or Iopromide (370 mgI/mL, Schering, Erlangen, Germany) by using a power injector at a rate of 1.5-2.5 mL/s, and the dose of the contrast agents was 1.5 mL/kg. Images of the hepatic arterial phase, portal vein phase and equilibrium phase were acquired at 20, 60 and 120 s, respectively. Vascular reconstruction processing was performed using a commercially available workstation and software with interactive maximum-intensity-projection (MIP) and volume-rendering techniques. The slice thickness of reconstructed image for retrospective review was 3.0 mm.

Image analysis

Two experienced abdominal radiologists retrospectively reviewed the imaging features of FNH by consensus, who were unaware of the patient's clinical data and pathological results. The following imaging features were assessed: the number of FNH lesion, location, maximum

Table 1 The multi-slice computed tomography findings of the 12 pediatric focal nodular hyperplasia cases

Case	Sex/age (yr)	Location/size (cm × cm)	Margin	Central scar	Fibrous septa	Pseudocapsule	Precontrast/HAP/PVP/EP	Spoke-wheel pattern	Draining vein
1	M/18	S4/5.2 × 3.7	Well-circumscribed	+	+	-	Hypo/hyper/iso/iso	+	Hepatic vein
2	M/4	S5/4.3 × 3.2	Well-circumscribed	+	+	-	Hypo/hyper/hyper/iso	-	Hepatic vein
3	M/2	S5/5.5 × 5.2	Well-circumscribed	+	+	+	Hypo/hyper/hyper/slight hyper	+	Hepatic vein
4	F/14	S1/4.3 × 3.0	Well-circumscribed	-	+	-	Hypo/hyper/iso/iso	+	Not identified
5	M/16	S5,S6/ 12.9 × 10.1	Well-circumscribed	+	+	-	Hypo/hyper/hyper/iso	+	Hepatic vein
6	F/4	S4/4.5 × 3.7	Well-circumscribed	+	+	-	Slight hypo/hyper/hyper/ iso	+	Hepatic vein
7	M/16	S6,S7/4.1 × 3.2	Well-circumscribed	-	-	-	Slight hypo/hyper/iso/iso	-	Not identified
8	F/16	S4/5.5 × 3.8	Well-circumscribed	+	+	-	Slight hypo/hyper/iso/iso	+	Hepatic vein
9	M/16	S6/6.5 × 5.2	Ill-defined margin	+	+	-	Hypo/hyper/iso/iso	+	Hepatic vein
10	F/17	S6/4.2 × 3.6	Ill-defined margin	+	+	-	Hypo/hyper/iso/iso	+	Not identified
11	M/18	S7/4.0 × 4.0	Well-circumscribed	+	+	-	Hypo/hyper/hyper/iso	+	Not identified
12	M/4	S8/4.8 × 4.5	Well-circumscribed	+	+	-	Slight hypo/hyper/iso/iso	-	Hepatic vein

HAP: Hepatic arterial phase; PVP: Portal venous phase; EP: Equilibrium phase; M: Male; F: Female.

axial diameter, margin, density of the lesions on the pre-contrast images and contrast-enhanced CT images, central scar, fibrous septa, pseudocapsule, the morphology of the feeding artery, and the presence of draining vessels (portal vein or hepatic vein). Other associated lesions in the liver were also recorded, such as hepatic adenomas and hemangiomas. Compared to the surrounding liver parenchyma, the density of FNH was classified as hypo-, iso-, or hyperdense on CT images. Homogeneous enhancement was considered if consistent enhancement was observed in all parts of the lesions, with the exception of the central scars and fibrous septa. The central scar was defined as the area in or near the center of the lesion that showed a significantly different density on pre-contrast or contrast enhanced CT images when compared to the surrounding component of the lesion. Fibrous septa were defined as the linear structures that radiated from the center to the periphery of the lesions.

RESULTS

The 12 cases of FNH were solitary lesions with a maximum lesion diameter of 4.0-12.9 cm and an average maximum diameter of 5.5 ± 2.5 cm. Out of the 12 cases of FNH, 2 cases (cases 3 and 5) had an exophytic growth. No hemorrhage, necrosis or calcification was observed in the FNH lesions. The detailed MSCT findings of the 12 FNH cases are listed in Table 1. Most FNH (10/12, 83.3%) had a well-defined margin. Central scar (10/12, 83.3%) and fibrous septa (11/12, 91.7%) were commonly detected in the pediatric cases of FNH (Figures 1-3). The central scar was found to be isodense (n = 7) or hypodense (n = 3) on pre-contrast CT images and was hypodense in the arterial phase. The central scar showed progressive enhancement, and became isodense in the portal vein phase (n = 2) and in the equilibrium phase (n = 8). However, the central scar was still hypodense in other two cases in the equilibrium phase. Fibrous septa were isodense on pre-contrast CT images, hypodense in the arterial phase images, and isodense in the portal vein phase and equilibrium phase images. Pseudocapsule was very rare in the cases of pediatric FNH (1/12, 8.3%) and was confirmed pathologically as the surrounding displaced veins, showing a hyperdense rim enhancement in the equilibrium phase.

All 12 cases of FNH were hypodense on pre-contrast scans, and were homogenously enhanced in all phases of the enhanced scans with the exception of the central scars and fibrous septa. FNH was significantly hyperdense in the arterial phase (12/12, 100%), and most of them were isodense in the portal vein phase (7/12, 58.3%) and equilibrium phase (11/12, 91.7%) (Figures 1A-D, 2A-D and 3A-D). The central feeding arteries in the FNH lesions were observed on CTA images in the arterial phase in all 12 cases of pediatric FNH (Figures 1B, 2B and 3C). However, no neovascularization of malignant tumors was observed. In 9 cases (75.0%), spoke-wheel shaped angioarchitecture of FNH was observed, with the feeding vessels radiating peripherally from the center and tapering gradually, suggesting a centrifugal blood supply of the tumors (Figures 1E, 2E and 3F). In 8 cases of FNH, the draining vessels of FNH entered the hepatic vein instead of the portal vein (Figures 1F and 2F). The draining vessels of the other 4 cases of FNH were not observed on CTA images in the portal vein phase or equilibrium phase.

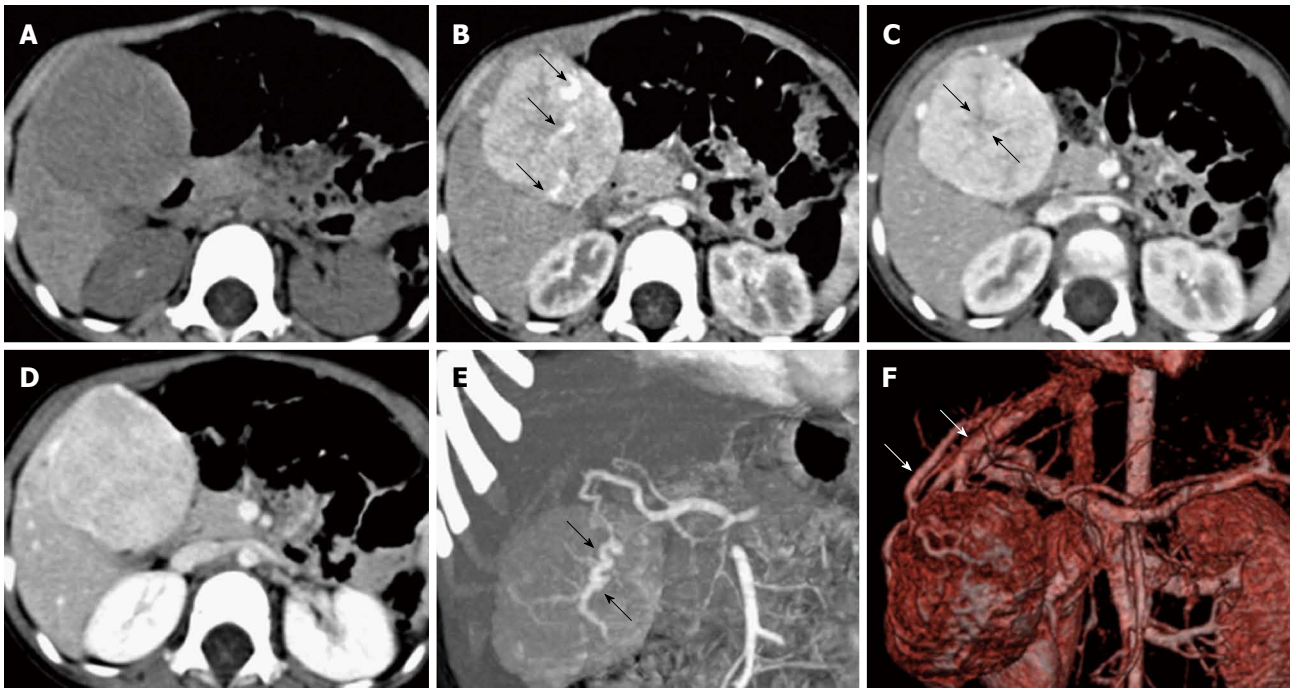

Figure 1 Focal nodular hyperplasia in a 2-year-old boy. A: The lesion was hypodense on pre-contrast computed tomography scan; B: The lesion was significantly enhanced in the arterial phase with enlarged feeding arteries (arrows); C: The lesion was hyperdense in the portal vein phase with hypodense central scar (arrows) and fibrous septa; D: The lesion was isodense in the equilibrium phase, and the scar shows delayed enhanced; E: Computed tomography angiography (CTA) in the arterial phase showed that the enlarged feeding artery was distorted with a spoke-wheel shaped blood supply (arrows); F: CTA in the portal vein phase showed the draining vessels directly into the hepatic vein (arrows).

No associated hepatic adenoma or hemangioma was observed in the liver of the 12 pediatric cases of FNH. Only 1 case (case 3) was associated with hemangioma in other parts of the body.

DISCUSSION

Pediatric FNH is a rare entity, accounting for approximately 2% of hepatic tumors and 0.02% of all pediatric tumors[10]. The exact pathogenesis of FNH is unclear; although it might be a proliferative response to intrahepatic vascular malformations[2]. Many studies have shown that the incidence of FNH increases after chemotherapy or radiotherapy for the treatment of solid tumors in children, suggesting that anti-tumor therapy-induced intrahepatic vascular injury may be risk factor for the development of FNH[4,11-13]. Current molecular pathological data revealed an activation of the β-catenin pathway, a marked upregulation of angiopoietin-1 and downregulation of angiopoietin-2 in FNH[14].

Most of the studies show that FNH in children is more common in females[4,6]. In a large series of 172 cases of pediatric FNH, Lautz *et al*[6] found that 66% (113/172) of the cases occurred in females. However, the majority of our cases were males, with a male to female ratio of 2:1. The high male to female ratio may be due to the bias inherent in the choice of cases enrolled in our study. All cases enrolled in this study were instances of FNH that had been confirmed by surgical resection or biopsy, and cases that were diagnosed by imaging modalities and close follow-up were not included. There are no specific clinical manifestations for FNH in children. The majority of the cases of FNH are usually discovered accidentally for unrelated reasons, with only 36% of cases showing symptoms[6]. The common symptoms of pediatric FNH include palpable abdominal mass and abdominal pain. Tumor rupture and hemorrhage are rare[4]. Laboratory test results often do not show clinical significance, and tumor markers such as AFP are usually in normal range[4].

After review the clinical features of 172 cases of pediatric FNH, Lautz *et al*[6] found an interesting result: pediatric FNH patients with a history of malignancy were significantly less likely to be symptomatic (12% *vs* 45%, $P < 0.0001$), were much smaller in size (2.8 ± 2.2 cm *vs* 8.0 ± 3.3 cm, $P < 0.0001$), and fewer patients required resection of the lesions (10% *vs* 78%, $P < 0.0001$) as compared with patients without a malignancy history. The pediatric FNH patients with a history of malignancy were more likely to have multiple FNH nodules and less likely to have central scars. In contrast, pediatric patients without a history of malignant lesions generally had larger FNH nodules and were more likely to have central scars[15,16]. The 12 patients in this group had no history of malignancy and had the features mentioned above: solitary FNH nodule, relatively large size (an average of 5.5 ± 2.5 cm), and high proportion of central scars (10/12, 83.3%).

Adult FNH patients may have associated hepatic adenomas (3.6%-6%) and hemangiomas (17%-23%)[2,3,17].

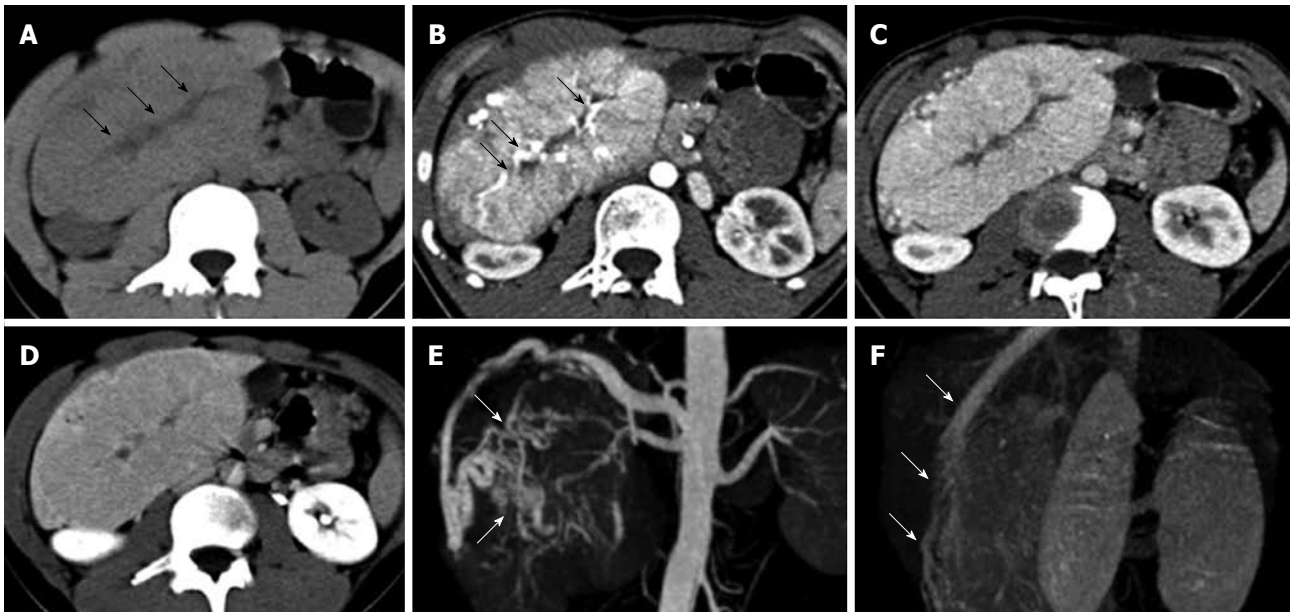

Figure 2 Focal nodular hyperplasia in a 16-year-old boy. A: The lesion was hypodense on pre-contrast computed tomography scan, and central scar with much lower density were identified (arrows); B: The lesion was significantly enhanced in the arterial phase with enlarged feeding arteries penetrating into the central scar (arrows); C: The lesion was slightly hyperdense in the portal vein phase; D: The lesion was isodense in the equilibrium phase with delayed enhancement of the central scar; E: Computed tomography angiography (CTA) in the arterial phase showed that the enlarged feeding arteries were distorted, and exhibited a spoke-wheel shaped blood supply (arrows); F: CTA in the portal vein phase showed the draining hepatic vein (arrows).

However, in our group of pediatric patients, there were no instances of associated hepatic adenomas or hemangiomas. More studies are needed to see whether FNH in adults and children differs in this respect.

The imaging appearances of FNH in pediatric patients on MSCT images reflect its pathological features. A typical case of FNH has the following pathological characteristics: well-differentiated hepatocytes forming nodules subdivided by fibrous septa, proliferation of ductules and malformed blood vessels in the central scars and fibrous septa, and no fibrous capsule[4]. The fibrous septa are the linear structures that radiate from the central scar to the periphery of the lesions and can sometimes be detected in the absence of a central scar. The hypodense fibrous septa were clearly depicted by CT in the arterial phase, and become isodense with the surrounding component of nodules in the portal vein and equilibrium phases. The sign of fibrous septa is a characteristic finding of FNH, and has not been reported in other tumors of the liver. However, after analyzing 78 cases of FNH using an obsolete spiral CT scanner with thick slice thickness (slice thickness of 5-7 mm), Brancatelli *et al*[17] found that only 8% of the patients showed this feature. Our results showed that, by using thin-slice MSCT imaging (slice thickness of 3.0 mm), this feature can be commonly observed (11/12, 91.7%). Kamel *et al*[1] suggest that this finding is best seen on volume-rendered images of the portal venous phase, and frequently detected with fine manipulation of the degree of tissue opacity of the volume-rendered images. However, the subtle changes of fibrous septa on volume-rendered images are difficult to detect in our experience.

The vascular central stellate scar is another pathological characteristic of FNH. The CT findings of the central scar in pediatric FNH are consistent with those of the central scar in adult FNH: compared to the surrounding nodules, the central scar was either hypodense or isodense on pre-contrast CT images, hypodense in the arterial phase (90%), and hypodense (68%) or isodense (22%) in the portal vein phase[17]. Due to the retention of contrast material within the myxoid matrix of the central scar, the scars show delayed contrast enhancement in the imaging scans at 5-20 min[17]. The central scar can be seen in 42.1%-50.0% of FNH nodules[17-19]. However, it was more common in the 12 pediatric cases of FNH in our group (10/12, 83.3%). This discrepancy could be explained by the larger diameter of the lesions (average 5.5 ± 2.5 cm) observed in our group of FNH, since detection of a central scar is clearly related to the size of the FNH (central scars are identified in only 35% of FNH ≤ 3.0 cm but in 65% of FNH > 3.0 cm)[17]. In addition to FNH, the central scar has also been described in fibrolamellar hepatocellular carcinoma (HCC) and large hemangiomas. A central scar width greater than 2 cm is helpful in differentiating between these three entities, since it is often detected in fibrolamellar HCC and sometimes in large hemangiomas, however never seen in FNH[20]. The presence of delayed contrast enhancement of the central scar and radiating fibrous septa were not statistically significant for the identification of these three entities[20].

With the development of CT software and hardware technology, the spatial and temporal resolutions of the images have significantly improved, which enables high-resolution CTA images possible. The post-processed high-resolution CTA images provide unique insights into the angioarchitecture of FNH. Although the hemodynamic

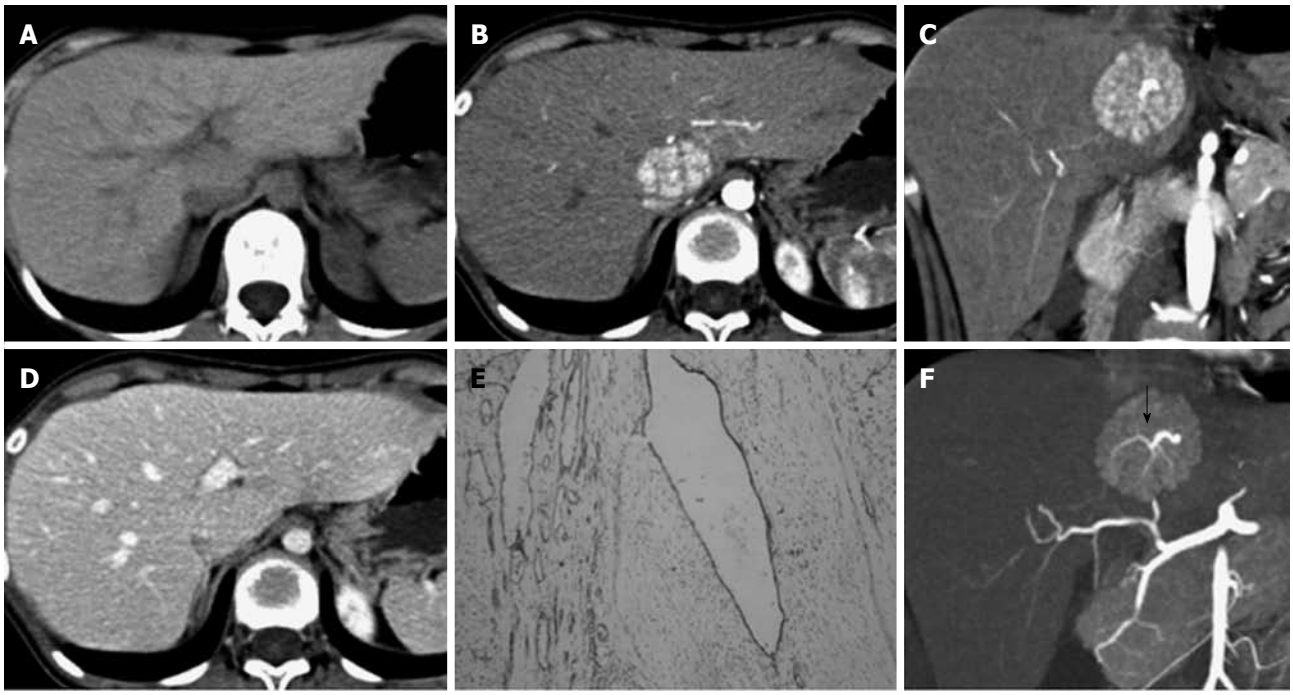

Figure 3 Focal nodular hyperplasia in a 14-year-old girl. A: The lesion was hypodense on pre-contrast computed tomography image; B, C: The lesion was significantly enhanced in the arterial phase with hypodense fibrous septa; D: The lesion was isodense in the portal vein phase; E: Immunohistochemical staining of CD34 revealed the abnormal blood vessels within fibrous septa (× 100); F: Computed tomography angiography in the arterial phase showed that a spoke-wheel shaped blood supply of the focal nodular hyperplasia (arrow).

characteristics of FNH (such as one or more enlarged feeding arteries entering into the center of the tumor and radiating to the periphery, a spoke-wheel shaped centrifugal blood supply) could be observed through the use of the invasive and time-consuming process of transcatheter angiography, it can also be non-invasively depicted on three-dimensional CTA images. Liu *et al*[18] compared CTA in 28 cases of FNH and 75 cases of other hypervascular hepatic tumors (hepatocellular carcinoma, hemangioma, and hepatic adenoma), using 16-MSCT with the MIP imaging and volume rendering technology. They found that the centrifugal arterial supply pattern was only seen in FNH, and this finding will assist in differentiating FNH from other hypervascular hepatic tumors. The three-dimensional display of the feeding artery provided by CTA may be valuable in planning for embolization or ligation of vessels in symptomatic pediatric FNH patients.

CTA can clearly show the draining vessels of pediatric FNH. FNH lesion exclusively drains into the hepatic vein branches either directly or *via* perinodular sinusoids[21,22]. HCC is drained almost always into the portal vein, only 1.8% of HCC draining into the hepatic vein. The identification of the draining blood vessels is therefore a reliable criterion for the differentiation between HCC and FNH[22].

FNH has no fibrous capsule and shows a well-defined margin on contrast-enhanced CT images in arterial phase. However, pseudocapsules can be detected in 8%-36% of FNH on CT images, which appearing as hypodense rims in the arterial phase and hyperdense rims in the portal vein phase and the delayed phase. This sign is especially obvious in large lesions, and may be a result of dilated surrounding vessels or sinusoids or compressed liver parenchyma[1,2,17]. The sign of pseudocapsule is also visible on magnetic resonance imaging (MRI) (9% of FNH in pre-contrast scanning and 18% in contrast enhanced scanning)[2]. Tumor capsule is a specific sign of HCC and is present in 60%-80% of cases. The capsule of HCC is mainly composed of fibrotic tissue and appears hypointense on both T1W and T2W images, whereas the pseudocapsule of FNH is hyperintense on T2W[23]. This discrepancy might help to differentiate between these two entities.

The enhancement pattern of pediatric FNH on multiphase CT images typically shows as early homogeneous enhancement (with the exception of the central scar and fibrous septa) in the arterial phase, hyperdense or isodense in the portal vein phase, and isodense in the equilibrium phase. These findings are consistent with the enhancement pattern of adult FNH reported in the literature[17].

If all of the imaging characteristics of FNH are identified on CT images, FNH can be diagnosed with confidence. However, approximately 50% of FNH lesions lacking typical imaging manifestations, especially the small lesions, are reported in the literature, such as the absence of central scar, rapid washout of contrast agents in the portal vein phase, absence of delayed enhancement in the central scar, and presence of rim enhancement of the pseudocapsule[3,4]. In these circumstances, it is necessary to distinguish FNH from other pediatric solid hypervascular tumor, and percutaneous fine needle biopsy

may be suggested when necessary. The malignant hepatic tumors, such as hepatoblastoma and hepatocellular carcinoma, manifest with elevated AFP, and heterogeneous density on CT images due to hemorrhage, necrosis and calcification, which are helpful for distinguishing these malignant tumors from FNH[4]. MRI examinations with hepatobiliary-specific gadolinium-based contrast agents (specifically gadobenate dimeglumine, gadoxetate disodium or gadoxetic acid) may be valuable for the diagnosis of FNH, particularly on the delayed hepatobiliary phase of imaging where FNHs are usually iso- or hyperintense relative to the liver parenchyma but rarely hypointense, presumably because of the presence of functioning hepatocytes and focal abnormal biliary excretion[24]. Hepatic adenoma in children is usually accompanied by glycogen storage disease and is prone to having multiple lesions and hemorrhage. Hepatic adenomas usually have no central scar and show heterogeneous density due to intratumoral hemorrhage. In the arterial phase, the CT attenuation values and relative enhancement of the lesion were significantly higher in FNH than in hepatic adenoma ($P < 0.05$). A threshold value of 1.6 for relative enhancement of the lesion in the arterial phase seems to be valuable to distinguish FNH from hepatic adenoma with an accuracy of 96%[25]. FNH has a centrifugal and spoke-wheel shaped blood supply, whereas hepatic adenoma has centripetal and subcapsular feeding blood supply[25]. Infantile hemangioendothelioma, or infantile hepatic hemangioma, is a benign vascular tumor that is unique to pediatric patients. Punctate calcification is seen in 50% of these cases[4]. The enhancement features are similar to those of adult hepatic hemangioma: intense peripheral nodular or corrugated enhancement in the arterial phase, and progressive centripetal fill-in of contrast material in the portal venous and delayed phase, which are different from those of FNH[4].

In summary, FNH in children manifests as solitary large nodule. The thin-slice MSCT images (slice thickness of 3.0 mm) facilitate in revealing the fibrous septa and central scar within FNH nodules. Multi-phase enhanced scanning has the capacity to demonstrate the enhancement characteristics of pediatric FNH: except for fibrous septa and central scars, FNH is homogenously enhanced in the arterial phase, and it appears isodense or hyperdense in the portal vein phase and isodense in the equilibrium phase. CTA provides unique insight into the hemodynamic of FNH: the enlarged feeding arteries in the center of the nodules, the spoke-wheel shaped and centrifugal blood supply, and the drainage into the hepatic vein. For asymptomatic pediatric FNH patients with typical MSCT imaging findings, unnecessary surgical resection can be avoided and close follow-up may be suggested. For pediatric FNH patients who cannot definitely be diagnosed by MSCT, further invasive and expensive tests, such as biopsy or surgical resection, are required.

ACKNOWLEDGMENTS

We would like to thank Ms. Caulloo-Dosieah Malini for assisting in English editing of our manuscript.

COMMENTS

Background

Hepatic focal nodular hyperplasia (FNH) is the second most common benign liver tumor after hemangioma in adult, whereas it is rare in children. It is important to differentiate FNH from other malignant lesions to avoid unnecessary surgical resection in pediatric patients. Since FNH is a slow growing tumor without malignant transformation and is rarely accompanied by the complications of hemorrhage or rupture, conservative "wait and see" strategy is recommended for asymptomatic children.

Research frontiers

Multi-slice computed tomography (MSCT) features a fast scanning speed and is ideal for assessing hepatic lesions in pediatric patients. With MSCT, dynamic multi-phase scanning is allowed in a very short period of time, and increased detection and characterization of focal liver lesion can be achieved. In addition, MSCT makes high-quality two- or three-dimensional vascular reconstruction images possible. There are few reports on the imaging features of FNH in children, especially the angioarchitecture of pediatric FNH on computed tomography angiography.

Innovations and breakthroughs

Twelve pediatric patients with FNH were reported in this study, and their MSCT features were reviewed. This study showed that central scar and fibrous septa were commonly found in children with FNH. Central scar was either isodense or hypodense on pre-contrast computed tomography (CT) images and showed progressive enhancement in the equilibrium phase. Fibrous septa were linear hypodense areas in the arterial phase and isodense in the portal and equilibrium phases. With the exception of central scars and fibrous septa within the lesions, pediatric FNH were homogenously enhanced on the contrast-enhanced CT images, and usually isodense in the portal venous phase and equilibrium phase. Central feeding arteries inside the tumors and a spoke-wheel shaped centrifugal blood supply were usually observed on computed tomography angiography (CTA) images. The characteristic imaging appearances on MSCT and CTA could reflect the pathological and hemodynamic features of pediatric FNH.

Applications

The study results suggest that dynamic multi-phase MSCT and CTA imaging is an effective method for diagnosing FNH in children.

Terminology

MSCT features a fast scanning speed (the time required for a single tube rotation is sub-second), and allows dynamic multi-phase scanning in a very short period of time. The ability of MSCT to acquire data with "isotropic voxel" makes high-quality two- or three-dimensional vascular reconstruction images possible.

Peer review

This manuscript is well written, and the authors retrospectively analyze the imaging features of FNH in children by MSCT and CTA, and suggested that it is an effective method for diagnosing FNH in children.

REFERENCES

1 **Kamel IR**, Liapi E, Fishman EK. Focal nodular hyperplasia: lesion evaluation using 16-MDCT and 3D CT angiography. *AJR Am J Roentgenol* 2006; **186**: 1587-1596
2 **Vilgrain V**. Focal nodular hyperplasia. *Eur J Radiol* 2006; **58**: 236-245
3 **Winterer JT**, Kotter E, Ghanem N, Langer M. Detection and characterization of benign focal liver lesions with multislice CT. *Eur Radiol* 2006; **16**: 2427-2443
4 **Chung EM**, Cube R, Lewis RB, Conran RM. From the archives of the AFIP: Pediatric liver masses: radiologic-pathologic correlation part 1. Benign tumors. *Radiographics* 2010; **30**: 801-826
5 **Yang Y**, Fu S, Li A, Zhou W, Pan Z, Cui L, Huang G, Wu B, Wu M. Management and surgical treatment for focal nodular hyperplasia in children. *Pediatr Surg Int* 2008; **24**: 699-703
6 **Lautz T**, Tantemsapya N, Dzakovic A, Superina R. Focal nodular hyperplasia in children: clinical features and current management practice. *J Pediatr Surg* 2010; **45**: 1797-1803

7 **Okada T**, Sasaki F, Kamiyama T, Nakagawa T, Nakanishi K, Onodera Y, Itoh T, Todo S. Management and algorithm for focal nodular hyperplasia of the liver in children. *Eur J Pediatr Surg* 2006; **16**: 235-240

8 **Cheon JE**, Kim WS, Kim IO, Jang JJ, Seo JK, Yeon KM. Radiological features of focal nodular hyperplasia of the liver in children. *Pediatr Radiol* 1998; **28**: 878-883

9 **Das CJ**, Dhingra S, Gupta AK, Iyer V, Agarwala S. Imaging of paediatric liver tumours with pathological correlation. *Clin Radiol* 2009; **64**: 1015-1025

10 **Reymond D**, Plaschkes J, Lüthy AR, Leibundgut K, Hirt A, Wagner HP. Focal nodular hyperplasia of the liver in children: review of follow-up and outcome. *J Pediatr Surg* 1995; **30**: 1590-1593

11 **Sugito K**, Uekusa S, Kawashima H, Furuya T, Ohashi K, Inoue M, Ikeda T, Koshinaga T, Tomita R, Mugishima H, Maebayashi T. The clinical course in pediatric solid tumor patients with focal nodular hyperplasia of the liver. *Int J Clin Oncol* 2011; **16**: 482-487

12 **Masetti R**, Biagi C, Kleinschmidt K, Prete A, Baronio F, Colecchia A, Festi D, Pession A. Focal nodular hyperplasia of the liver after intensive treatment for pediatric cancer: is hematopoietic stem cell transplantation a risk factor? *Eur J Pediatr* 2011; **170**: 807-812

13 **Sudour H**, Mainard L, Baumann C, Clement L, Salmon A, Bordigoni P. Focal nodular hyperplasia of the liver following hematopoietic SCT. *Bone Marrow Transplant* 2009; **43**: 127-132

14 **Maillette de Buy Wenniger L**, Terpstra V, Beuers U. Focal nodular hyperplasia and hepatic adenoma: epidemiology and pathology. *Dig Surg* 2010; **27**: 24-31

15 **Towbin AJ**, Luo GG, Yin H, Mo JQ. Focal nodular hyperplasia in children, adolescents, and young adults. *Pediatr Radiol* 2011; **41**: 341-349

16 **Do RK**, Shaylor SD, Shia J, Wang A, Kramer K, Abramson SJ, Price AP, Schwartz LH. Variable MR imaging appearances of focal nodular hyperplasia in pediatric cancer patients. *Pediatr Radiol* 2011; **41**: 335-340

17 **Brancatelli G**, Federle MP, Grazioli L, Blachar A, Peterson MS, Thaete L. Focal nodular hyperplasia: CT findings with emphasis on multiphasic helical CT in 78 patients. *Radiology* 2001; **219**: 61-68

18 **Liu YJ**, Fan WJ, Yuan ZD, Liu PC, Wang CR, Yan WQ, Wang SM, Chen JH, Liu Z. Research on focal nodular hyperplasia with MSCT and postprocessing. *World J Gastroenterol* 2009; **15**: 4838-4843

19 **Johnson PT**, Zaheer A, Anders R, Fishman EK. Dual-phase computed tomographic angiography of focal nodular hyperplasia: defining predictable postcontrast attenuation levels relative to aorta and inferior vena cava. *J Comput Assist Tomogr* 2010; **34**: 720-724

20 **Blachar A**, Federle MP, Ferris JV, Lacomis JM, Waltz JS, Armfield DR, Chu G, Almusa O, Grazioli L, Balzano E, Li W. Radiologists' performance in the diagnosis of liver tumors with central scars by using specific CT criteria. *Radiology* 2002; **223**: 532-539

21 **Miyayama S**, Matsui O, Ueda K, Kifune K, Yamashiro M, Yamamoto T, Komatsu T, Kumano T. Hemodynamics of small hepatic focal nodular hyperplasia: evaluation with single-level dynamic CT during hepatic arteriography. *AJR Am J Roentgenol* 2000; **174**: 1567-1569

22 **Brancatelli G**, Federle MP, Katyal S, Kapoor V. Hemodynamic characterization of focal nodular hyperplasia using three-dimensional volume-rendered multidetector CT angiography. *AJR Am J Roentgenol* 2002; **179**: 81-85

23 **Hussain SM**, Terkivatan T, Zondervan PE, Lanjouw E, de Rave S, Ijzermans JN, de Man RA. Focal nodular hyperplasia: findings at state-of-the-art MR imaging, US, CT, and pathologic analysis. *Radiographics* 2004; **24**: 3-17; discussion 18-19

24 **Gupta RT**, Iseman CM, Leyendecker JR, Shyknevsky I, Merkle EM, Taouli B. Diagnosis of focal nodular hyperplasia with MRI: multicenter retrospective study comparing gadobenate dimeglumine to gadoxetate disodium. *AJR Am J Roentgenol* 2012; **199**: 35-43

25 **Ruppert-Kohlmayr AJ**, Uggowitzer MM, Kugler C, Zebedin D, Schaffler G, Ruppert GS. Focal nodular hyperplasia and hepatocellular adenoma of the liver: differentiation with multiphasic helical CT. *AJR Am J Roentgenol* 2001; **176**: 1493-1498

S- Editor Gou SX **L- Editor** A **E- Editor** Zhang DN